^{129}Xe NMR study of 12-tungstophosphoric heteropoly acid supported on silica ☆

V.V. Terskikh [a,1], V.M. Mastikhin †, M.N. Timofeeva, L.G. Okkel' and V.B. Fenelonov

Boreskov Institute of Catalysis, Novosibirsk 630090, Russia
[a] E-mail: tersk@catalysis.nsk.su

Received 9 May 1996; accepted 14 August 1996

The structure of 12-tungstophosphoric heteropoly acid ($H_3PW_{12}O_{40}$) supported on silica has been studied by ^{129}Xe NMR of adsorbed xenon. The ^{129}Xe NMR spectra are found to depend on the surface HPA concentration. The ^{129}Xe NMR data provide evidence for the presence of an organized microporous structure within HPA overlayers. These results are in agreement with nitrogen adsorption and capillary condensation (77 K) measurements. The high sensitivity of the ^{129}Xe NMR method and its applicability for testing of silica-based HPA catalysts are demonstrated.

Keywords: heteropoly acid; silica; ^{129}Xe NMR; adsorbed xenon; microporosity

1. Introduction

Heteropoly oxometallates have been widely used in heterogeneous catalysis. Their acidic forms (heteropoly acids, HPA) are applied for acid type reactions while their cationic exchanged derivatives (heteropoly salts) are active in acidic and oxidation catalytic reactions [1–4]. The NH_4^+, Cs^+ and Rb^+ salts are known to have high (> 100 m^2/g) surface areas and developed microporous structures [5–8]. The major influence of the porosity on the catalytic properties of such compounds is associated with the possibility to perform "bulk-type" and/or "surface-type" reactions [2,8]. In contrast, heteropoly acids have little or no porosity. Because of their low surface the heteropoly acids themselves are usually dispersed over neutral high-area supports. The nature of the support and the HPA loading have a profound effect on the activity and stability of these catalysts.

Electron microscopy, X-ray and NMR (^{1}H and ^{31}P MAS) studies of the HPA/SiO_2 catalysts have revealed three types of surface HPA species depending upon HPA loading [9,10]. At low HPA content (< 20 wt%) there are mainly highly dispersed particles with size smaller then 15 Å. They are, probably, isolated HPA molecules attached to silica surface (HPA-I). At > 20 wt% of HPA content the clusters with size ca. 50 Å and irregular crystalline structure can be detected (HPA-II). Finally, at 40–50 wt% content, the large HPA crystals and/or polycrystallites with size > 500 Å are found (HPA-III).

Nowadays main information on the microporous structure of solids is usually obtained by appropriate analyses of nitrogen adsorption (77 K) isotherms. Nevertheless, one should keep in mind the limitations of this conventional technique. It has been shown that nitrogen may be unsuitable for measurements of microporosity because of the strong interaction of nitrogen with the solids due to the large quadrupole moment of nitrogen [11]. The lack of significant microporosity for some solids can be ascribed to the fact that pores cannot accommodate the nitrogen molecule at 77 K. The development of a new method which would provide independent information on the microporosity seems to be useful.

In the last few years, ^{129}Xe NMR spectroscopy of adsorbed xenon has been extensively employed as a powerful technique to characterize the porous structure of microporous materials, particularly zeolites. Due to the large polarizability of the xenon atoms (free diameter 4.4 Å) the ^{129}Xe NMR chemical shift of xenon was found to be very sensitive to its local environment. In ref. [12] an empirical correlation between the xenon chemical shift and the void space of zeolites has been proposed. Refs. [13–15] contain reviews on the basic features and limitations of this technique and its application for microporous solids.

Recently, the ^{129}Xe NMR method has been used for a comparative study of the microporosity of heteropoly salts [16]. The ^{129}Xe NMR results confirmed the presence of a homogeneous and organized porous structure for solid heteropoly ammonium, potassium and cesium salts of 12-tungstophosphoric, 12-molybdophosphoric and 12-tungstosilicic acids which a priori are known to have a high surface area.

Here we report the results of the first ^{129}Xe NMR

☆ A preliminary report of this work was presented to the Second European Congress on Catalysis EUROPACAT-II, Maastricht, The Netherlands, 3–8 September 1995.

[1] To whom correspondence should be addressed.

† Deceased.

study of HPA/SiO$_2$ catalysts upon variation of HPA loading and sample pretreatment conditions. These results are combined with the data on porosity of the same samples measured by nitrogen adsorption and capillary condensation.

2. Experimental

Chemical pure $H_3PW_{12}O_{40}$ was recrystallized from water. The samples of HPA supported on mesoporous SiO$_2$ (BET surface area 382 m^2/g) were prepared by impregnation of the support with an aqueous HPA solution, with subsequent drying at room temperature in a desiccator.

For NMR experiments xenon with the natural abundance of ^{129}Xe isotope (26%) was employed. Prior to the xenon adsorption the samples were evacuated for 16 h at 373 K in 10 mm o.d. NMR samples tubes with vacuum glass stopcock. Equilibrium xenon pressure was varied from 10 to 550 Torr at ambient temperature.

The ^{129}Xe NMR spectra were obtained on a Bruker MSL-400 NMR spectrometer (magnetic field 9.4 T) at a resonance frequency 110.6 MHz. The radiofrequency pulse width was 10 μs, delay between pulses 2 s. The number of accumulated spectra was typically from 500 to 3000. Chemical shifts were referenced to an external standard of low-pressure Xe gas with an accuracy ±1 ppm. All spectra are presented at the same vertical scale.

The pore structures were determined from nitrogen adsorption isotherms (77 K) in a Micromeritics ASAP 2400 equipment. The samples were outgassed at 373 K under vacuum before measurements. The pore size distributions were calculated from the desorption branch of isotherms in the range of capillary-condensation hysteresis by the Broeckhoff and De Boer method [17]. Micropore volumes were determined by the comparative method [18] which is a modification of the t-method [17].

3. Results and discussion

Fig. 1 shows the ^{129}Xe NMR spectra of xenon adsorbed on the initial SiO$_2$ and the HPA/SiO$_2$ catalysts with various HPA loading at the same equilibrium xenon pressure. The chemical shifts of adsorbed xenon as a function of the equilibrium pressure of xenon are displayed in fig. 2.

The ^{129}Xe NMR spectrum for the starting silica consists of one narrow line with the chemical shift of 69 ppm (fig. 1, a). This shift is independent of the equilibrium pressure (fig. 2, a).

In general, the ^{129}Xe NMR chemical shift of adsorbed xenon is the sum of the terms corresponding to the various perturbations affecting the xenon atom. With some simplification by analogy with the model suggested by Ito and Fraissard [13] under the conditions of fast xenon exchange the chemical shift can be expressed as

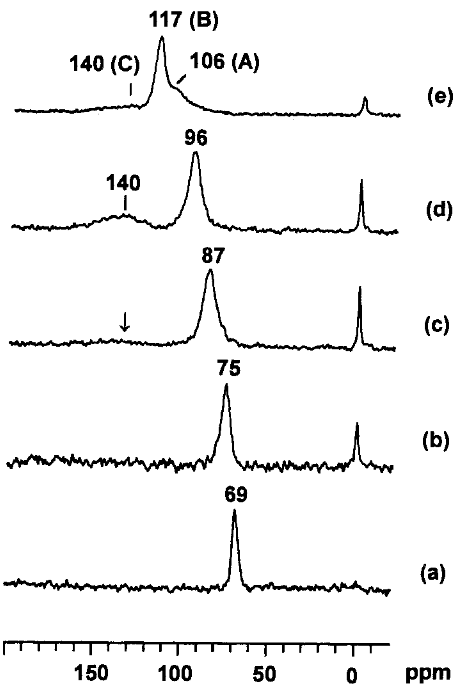

Fig. 1. Effect of HPA loading on ^{129}Xe NMR spectra of adsorbed xenon (equilibrium pressure 450 Torr, temperature 293 K): (a) SiO$_2$, (b) 5 wt% HPA/SiO$_2$, (c) 20 wt% HPA/SiO$_2$, (d) 40 wt% HPA/SiO$_2$, (e) 60 wt% HPA/SiO$_2$. The line at ~ 0 ppm belongs to the gaseous xenon between catalyst grains.

$$\delta = \sum \delta_i P_i , \qquad (1)$$

where δ_i is the chemical shift of state i and P_i the relative xenon population in this state, so that $\sum P_i = 1$.

For xenon adsorbed on the starting silica the chemical shift can be presented as

$$\delta = \delta_{SiO_2} P_{SiO_2} , \qquad (2)$$

where $P_{SiO_2} = 1$ and the chemical shift $\delta_{SiO_2} = 69$ ppm is independent of the xenon pressure (fig. 2, a) due to the rapid exchange of the adsorbed xenon with the gas phase in agreement with the previously reported data for silica gels [19,20]. According to the correlation between the chemical shift and mean pore diameter established in ref. [20] this shift corresponds to a value of 90 Å for the mean pore diameter of the silica support.

The xenon spectrum for the 5 wt% HPA/SiO$_2$ sample is shown in fig. 1, b. Supporting even of a small amount of HPA results in a notable increase of the xenon chemical shift and line width. Further increase of the HPA content results in an essential increase of these spectral parameters (fig. 1, c). A new broad line of small intensity at ca. 140 ppm appears. For 20 wt% HPA/SiO$_2$ the chemical shift decreases from 95 to 86 ppm while increasing the xenon pressure from 30 to 550 Torr (fig. 2, b).

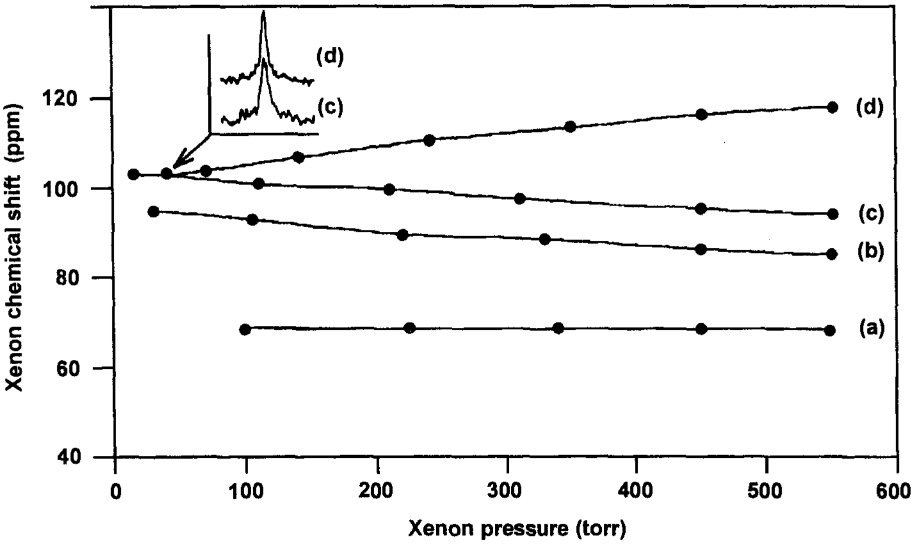

Fig. 2. Effect of xenon equilibrium pressure on the xenon chemical shift for supported HPA/SiO$_2$ catalysts: (a) SiO$_2$, (b) 20 wt% HPA/SiO$_2$, (c) 40 wt% HPA/SiO$_2$, (d) 60 wt% HPA/SiO$_2$ (line B). The spectra for 40 wt% HPA/SiO$_2$ (c) and 60 wt% HPA/SiO$_2$ (d) at xenon equilibrium pressure 40 Torr are inserted.

As it was noted in the Introduction, at low loading (< 20 wt%) the surface HPA species are mainly the isolated HPA molecules (HPA-I, fig. 3). The mesoporous structures of these samples should not change considerably compared to unloaded silica. The increased values of the xenon chemical shift detected are due to an interaction of xenon atoms with a limited number of strong adsorption sites apparently associated with surface HPA-I species. In this case, the xenon chemical shift can be described by the sum of two main contributions from xenon adsorbed on the silica surface and on HPA-I species. Under the conditions of fast exchange

$$\delta = \delta_{\mathrm{SiO_2}} P_{\mathrm{SiO_2}} + \delta_{\mathrm{HPA\text{-}I}} P_{\mathrm{HPA\text{-}I}} \,. \tag{3}$$

The increase of the HPA content from 1 to 20 wt% results in the increase of the xenon chemical shift (at the same equilibrium pressure) with an increase of the amount of HPA-I adsorption sites ($P_{\mathrm{HPA\text{-}I}}$ term). Such sites are occupied first and cause high initial value of the chemical shift. With increasing xenon pressure only the silica sites are available for xenon adsorption ($P_{\mathrm{SiO_2}}$ term). It results in a decrease of the average chemical shift with the equilibrium pressure, as was observed for the 20 wt% HPA/SiO$_2$ catalyst (fig. 2, b). The contribution to the chemical shift due to xenon–HPA-I interactions ($\delta_{\mathrm{HPA\text{-}I}}$) can be measured at low surface coverage, i.e. at low xenon pressure. For the 20 wt% sample the value of $\delta_{\mathrm{HPA\text{-}I}}$ is found to be 95 ppm.

At 40 wt% loading the HPA-II clusters with size ca. 50 Å are formed on the silica surface (HPA-II, fig. 3). In this case the xenon chemical shift is determined largely by two main interactions in which xenon is involved: adsorption on the silica surface and sorption by HPA-II species. We can rewrite eq. (1) as

$$\delta = \delta_{\mathrm{SiO_2}} P_{\mathrm{SiO_2}} + \delta_{\mathrm{HPA\text{-}II}} P_{\mathrm{HPA\text{-}II}} \,. \tag{4}$$

The behavior of the chemical shift of the narrower line in fig. 1, d with pressure (fig. 2, c) can be explained in the same way as for the previous sample. The chemical shift due to the interactions of xenon with HPA-II ($\delta_{\mathrm{HPA\text{-}II}}$) is markedly higher (103 ppm) than the value of $\delta_{\mathrm{HPA\text{-}I}}$. The broad line at 140 ppm becomes more pronounced.

For 60 wt% HPA/SiO$_2$ the xenon spectrum consists of three overlapping lines: at 106 (A), 117 (B) and

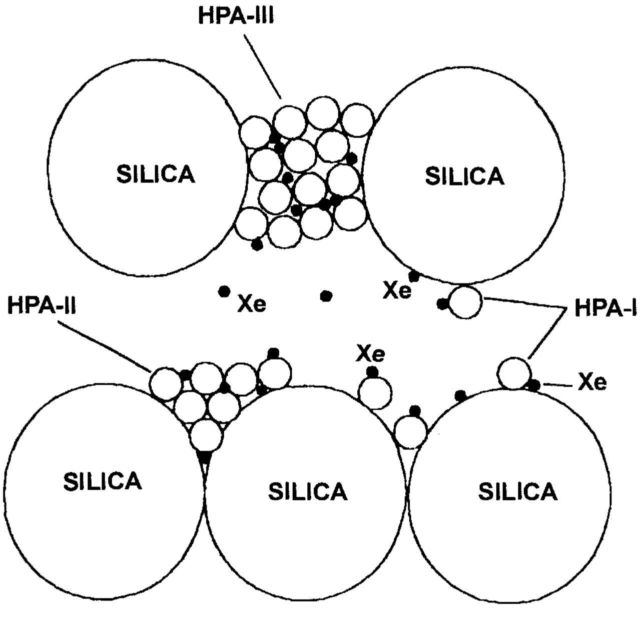

Fig. 3. Schematic representation of the sorbed and interporous xenon atoms in the pore structure of HPA/SiO$_2$ catalyst.

140 ppm (C) (fig. 1, e). Line A appears when the xenon pressure achieves 240 Torr. The chemical shift of this line decreases with increase of xenon pressure in the same way with 20 and 40% HPA/SiO$_2$ samples. The shift of line B increases with the xenon equilibrium pressure (fig. 2, d). A similar dependence of the xenon NMR shift is reported for zeolites and found to be caused by Xe–Xe collisions in micropores [13]. The observed increase of the chemical shift of xenon adsorbed on the 60 wt% sample seems to be due to the same reasons. In this case, the shift can be written in an expansion

$$\delta = \delta_{\mathrm{SiO_2}} P_{\mathrm{SiO_2}} + \delta_{\mathrm{HPA\text{-}III}} P_{\mathrm{HPA\text{-}III}} + \delta_{\mathrm{Xe\text{-}Xe}} P_{\mathrm{Xe}} , \qquad (5)$$

where an additional coefficient $\delta_{\mathrm{Xe-Xe}}$ is associated with Xe–Xe collisions while P_{Xe} is the local density of xenon adsorbed in the micropores of the sample. Therefore, the presence of micropores for 60 wt% HPA/SiO$_2$ sample is established by the xenon NMR data.

The presence of microporous free volumes within HPA overlayers is confirmed by nitrogen porosimetry of the same samples. Table 1 shows surface areas of mesopores (S), mesopore volumes (V_{p}), mean mesopore diameters ($D = 4V_{\mathrm{p}}/S$) and micropore volumes (V_μ) for the starting silica and the samples loaded with 1–60 wt% of HPA, as obtained from nitrogen adsorption and capillary condensation. Surface area and volume of mesopores both decrease with HPA loading. However, the mean diameter of mesopores does not change significantly. The pore size distributions for these samples are shown in fig. 4. The shapes of the distributions are subjected only to moderate changes. At the same time, the HPA supporting results in formation of micropores with diameter < 20 Å (table 1). The amount of micropores for the 60 wt% HPA/SiO$_2$ sample recalculated per gram of HPA (micropore surface $S_\mu = 68$ m^2/g and micropore volume $V_\mu = 0.032$ cm^3/g) is comparable with that for bulk ammonium salt of $(NH_3)_3PW_{12}O_{40}$ reported in ref. [5] ($S_\mu = 128$ m^2/g, $V_\mu = 0.050$ cm^3/g). At the same time, no microporosity was detected for bulk $H_3PW_{12}O_{40}$ in agreement with the data of refs. [5–7].

A number of workers clearly demonstrated that the xenon shift at low pressure is a measure of the dimension of the void space of zeolites. The correlation between this shift and the diameter of the zeolite cavities has been determined [12]. For the 60 wt% HPA sample the chemical shift of 103 ppm measured at low pressure should be attributed to the $\delta_{\mathrm{HPA\text{-}III}}$ term that is characteristic of collisions between xenon and the micropore wall of HPA-III. It is remarkable, that at low pressure the xenon spectra for 40 wt% HPA and 60 wt% HPA catalysts are very similar to each other (inset in fig. 2). If the microporous structure of the 60 wt% HPA/SiO$_2$ sample is assumed to be cylindrical, the mean diameter of such pores can be estimated from xenon data to be about 7 Å.

Table 1
Morphology of HPA/SiO$_2$ catalysts

Sample	S (m^2/g)	V_{p} (cm^3/g)	D (Å)	V_μ [a] (cm^3/g$_{\mathrm{SiO_2}}$)
SiO$_2$	375	1.040	111	0.0
1 wt% HPA/SiO$_2$	343	1.019	118	0.012
5 wt% HPA/SiO$_2$	322	0.946	117	0.013
15 wt% HPA/SiO$_2$	261	0.807	123	0.014
20 wt% HPA/SiO$_2$	231	0.720	124	0.016
40 wt% HPA/SiO$_2$	150	0.461	122	0.025
60 wt% HPA/SiO$_2$	82	0.204	94	0.048
HPA	8	0.017	–	0.0

[a] Micropore volumes are given in cm^3 per gram of the silica.

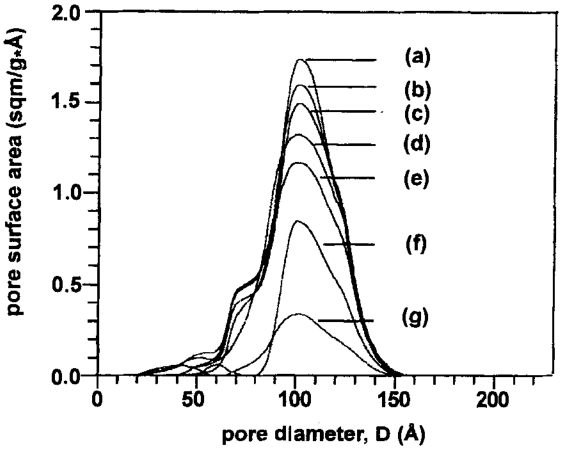

Fig. 4. Desorption pore size distributions (by the method of Broeckhoff and De Boer) for SiO$_2$ and supported HPA/SiO$_2$ catalysts: (a) SiO$_2$, (b) 5 wt% HPA/SiO$_2$, (c) 20 wt% HPA/SiO$_2$, (d) 40 wt% HPA/SiO$_2$, (e) 60 wt% HPA/SiO$_2$.

The similarity of the values of $\delta_{\mathrm{HPA\text{-}II}}$ and $\delta_{\mathrm{HPA\text{-}III}}$ is hand in hand with a similarity of the internal structure of the HPA overlayers formed at 40 and 60 wt% of loadings. Nevertheless, the difference of the size of the surface species for these two samples is reflected by xenon NMR data.

For 60 wt% HPA sample the microporosity is closed as for zeolites. The increase of the xenon loading results in the increase of the shift caused by Xe–Xe collisions within the porous framework. In contrast, for 40 wt% HPA sample an open microporosity is typical. Fast exchange of the sorbed xenon with the gas phase of the mesopores results in the chemical shifts which decrease with the equilibrium pressure. Indeed, the mean diameters of micropores in two cases are very similar (ca. 7 Å).

The nature of the microporosity of HPA overlayers on silica surface needs clarification. From the one hand the micropores can be contained within the high-dispersed HPA crystals and hence to be intrinsic of the bulk crystal structure of the HPA solids. From X-ray and neutron diffraction experiments [21] the diameter of the internal channels formed if crystal water is removed can be calculated as 4.8 Å that is close to the value of 7 Å from xenon data. At the same time no profound porosity accessible for xenon penetration was detected in our experiments for bulk 12-tungstophosphoric heteropoly acid since the xenon spectrum for this sample does not contain lines from adsorbed xenon. This is in agreement with the nitrogen porosimetry data. So, on the other hand these micropores can be ascribed to spaces between HPA crystallites, formed upon supporting. Such pores can occur as a result of aggregation rather than crystal structure effects.

The specific density (ρ) of the supported component can be calculated from the dependence of the mesopore volume (V_p) on the loading (X). This dependence is described by a linear equation,

$$V_p = V^0(1 - X) + X/\rho, \qquad (6)$$

where X is the HPA loading in g(HPA)/ g(HPA + SiO$_2$); and V^0 the initial mesopore volume (1.04 cm^3/g). For the studied HPA/SiO$_2$ catalysts the density of HPA overlayers was found to be 2.9 g/cm^3 in the wide range of X (0.01–0.60). This value is nearly twice smaller than that reported for bulk 12-tungstophosphoric acid, 5.6 g/cm^3 [21]. This result shows a considerable difference between the structure of the bulk and supported HPA particles. The latter seems to have an intrinsic microporosity and high disorder compared to bulk HPA.

Fig. 3 schematically depicts the possible scheme of the structure of HPA on silica surface.

The state of micropores is clearly evident from ^{129}Xe NMR spectra of xenon adsorbed on 60 wt% HPA/SiO$_2$ sample. Fig. 5 demonstrates the effect of the pretreatment conditions on the ^{129}Xe NMR spectra for this catalyst. The spectra were recorded at 293 K with equilibrium xenon pressure of 450 Torr in all the cases.

The spectrum of the untreated sample contains a line from adsorbed xenon at 52 ppm (fig. 5, a). This spectrum does not show strong interactions of Xe with surface HPA-III species that are covered by sorbed water molecules.

The evacuation of this sample at ambient temperature for 16 h results in the spectrum with a broad line at ca. 150 ppm and a line at 82 ppm (fig. 5, b). This treatment partially removes water molecules from the surface as well as from micropores. Two lines in the xenon spectrum for this sample are associated with two different Xe states. The narrower line at 82 ppm most likely belongs to xenon adsorbed on the surface of mesopores that includes silica and HPA regions. The broad line at ca. 150 ppm is caused by xenon penetrated into HPA species that partially lost water molecules from their microporous structure. The high value of the chemical shift is related to Xe–water collisions within the microporous medium. The water easily removed by evacuation is thought to be zeolitic.

The heating of this sample in vacuum at 373 K for 4 h results in the further removal of water from the microporous structure of the HPA species. This process is well illustrated by ^{129}Xe NMR spectra (fig. 5, c and d). The spectrum of xenon adsorbed on the sample evacuated at 373 K for 16 h contains of three overlapping components (fig. 5, d or fig. 1, e). The broad line at 140 ppm belongs to xenon atoms interacted with residual water molecules inside of HPA micropores. Such lines are also present in the xenon spectra of 20 wt% and 40 wt% HPA/SiO$_2$ samples (fig. 1, c and d).

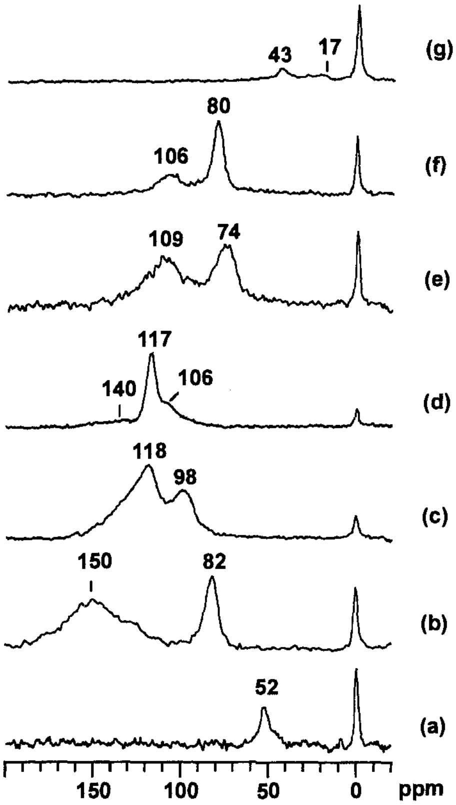

Fig. 5. ^{129}Xe NMR spectra of xenon adsorbed on 60 wt% HPA/SiO$_2$ sample (xenon equilibrium pressure 450 Torr, 293 K) after treatment: (a) evacuated at 293 K for 10 min, (b) sample (a) evacuated at 293 K for 16 h, (c) sample (b) evacuated at 373 K for 4 h, (d) sample (c) evacuated at 373 K for 12 h, (e) sample (c) after exposure to NH$_3$ (100 Torr, 348 K, 8 h with subsequent evacuation), (e) sample (d) after heating in air at 773 K for 1 h and evacuation, (f) sample (e) after calcination in air at 1073 K for 8 h and subsequent evacuation.

The lines A and B (fig. 1, e) correspond to xenon in two relatively isolated regions of the sample with slow diffusion exchange between them. Evidently there are surface HPA particles of different sizes. For large HPA-III species the line B is due to an absence of the noticeable exchange of xenon between the closed (more isolated) internal microporous and large mesoporous volumes. The value of the chemical shift of this line increases with the increase of xenon pressure and Xe–Xe collisions. The line A should be assigned to xenon atoms interacting with smaller clusters of HPA-II type. This line shifts to the high field with the increase of the xenon pressure due to an exchange of xenon between sorbed and gaseous states since the more open micropores of HPA-II species are directly connected with the silica mesopores. A similar dependence of the shift is found for the 40 wt% HPA/ SiO$_2$ sample. Indeed, for the 60 wt% HPA/SiO$_2$ catalyst there are HPA particles of different sizes as indicated by the spectrum with two overlapping components (A and B, fig. 1, e).

The exposure of this sample to NH_3 gas followed by evacuation results in a transformation of heteropoly acid species into heteropoly ammonia salt ones. The line at 109 ppm in the ^{129}Xe NMR spectrum (fig. 5, e) belongs to the xenon atoms within so formed porous issues of salt.

Further heating of this sample at 773 K in air for 1 h results in the decomposition of supported HPA species with production of HPA–PW-oxide compounds with a reduced microporosity. The major amount of xenon is adsorbed on the mesopore surface of this sample (line with the chemical shift of 80 ppm, fig. 5, f). The calcination of this sample in air at 1073 K for 8 h leads to the deep decomposition of HPA to the oxide compounds. This sample does not show any micropores. Moreover, the oxides block the silica pores which decreases its specific surface area and pore volume and leads to the set of unresolved xenon lines of small intensity from 17 to 43 ppm (fig. 5, g).

4. Conclusion

The results of the first application of ^{129}Xe NMR technique in studies of silica-based heteropoly acid catalysts are presented.

The types of surface species depend significantly upon the HPA loading, which is reflected by the ^{129}Xe NMR spectra of adsorbed xenon. ^{129}Xe NMR reveals the arrangement of high-dispersed HPA overlayers which in absence of water exhibit the developed microporous structure with the inherent pore diameter of ca. 7 Å. Two types of microporosity: "more closed" as that in zeolites and "more open" loosely connected with mesopores is found to depend on the surface HPA concentration and/or on the size of surface HPA crystallites. It is important to note that there are no available micropores for bulk HPA. It is the dispersion of HPA over high-surface silica supports that results in formation of micropores. This observation should be taken into account in studies of the catalytic properties of such catalysts.

The high sensitivity of the ^{129}Xe NMR technique allowed us to test the surface HPA overlayers upon the catalyst pretreatment conditions. This was well demonstrated for 60 wt% HPA/SiO_2 sample with step-by-step evacuation, exposure to ammonia and calcination.

Acknowledgement

This work was carried out with the financial support from the Russian Foundation for Basic Research (Grant 93-03-04774).

References

[1] Y. Ono, in: *Perspectives in Catalysis*, eds. J.M. Thomas and K.I. Zamaraev (Blackwell, London, 1992) p. 431.

[2] M. Misono, in: *Catalysis by Acids and Bases*, ed. B. Imelik (Elsevier, Amsterdam, 1985) p. 147.

[3] I.V. Kozhevnikov, Russ. Chem. Rev. 56 (1987) 811; 62 (1993) 473.

[4] M. Misono, Catal. Rev. 30 (1988) 339.

[5] J.B. McMonagle and J.B. Moffat, J. Colloid Interf. Sci. 101 (1984) 479.

[6] J.B. Moffat, J. Mol. Catal. 52 (1989) 169.

[7] G.B. McGarvey, N.G. Taylor, V.S. Nayak and J.B. Moffat, J. Mol. Catal. 80 (1993) 75.

[8] N. Essayem, G. Coudurier, M. Fournier and J.C. Vedrine, Catal. Lett. 34 (1995) 223.

[9] S.M. Kulikov, M.N. Timofeeva, I.V. Kozhevnikov, V.I. Zaikovsky, L.M. Plyasova and I.A. Ovsyannikova, Izv. Akad. Nauk SSSR, Ser. Khim. 4 (1989) 763.

[10] V.M. Mastikhin, S.M. Kulikov, A.V. Nosov, I.V. Kozhevnikov, I.L. Mudrakowskii and M.N. Timofeeva, J. Mol. Catal. 60 (1990) 65.

[11] A.F. Venero and J.N. Chiou, Mater. Res. Soc. Symp. Proc. 111 (1988) 235.

[12] J. Demarquay and J. Fraissard, Chem. Phys. Lett. 136 (1987) 314.

[13] J. Fraissard and T. Ito, Zeolites 8 (1988) 350.

[14] P.J. Barrie and J. Klinowski, Progress in NMR Spectroscopy 24 (1992) 91.

[15] D. Raftery and B.F. Chmelka, NMR Basic Principles and Progress 30 (1993) 111.

[16] J.L. Bonardet, J. Fraissard, G.B. McGarvey and J.B. Moffat, J. Catal. 151 (1995) 147.

[17] J.C.P. Broeckhoff and J.H. de Boer, J. Catal. 9 (1967) 10; 10 (1968) 391.

[18] A.P. Karnaukhov, V.B. Fenelonov and V.Yu. Gavrilov, Pure Appl. Chem. 61 (1989) 1913.

[19] W.C. Conner, E.L. Weist, T. Ito and J. Fraissard, J. Phys. Chem. 93 (1989) 4138.

[20] V.V. Terskikh, I.L. Mudrakovskii and V.M. Mastikhin, J. Chem. Soc. Faraday Trans. 89 (1993) 4239.

[21] G.M. Brown, M.R. Noe-Spirlet, W.R. Busing and H.A. Levy, Acta Cryst. B 33 (1977) 1038.